Phase Transitions in the Canted Antiferromagnet*

C. W. FAIRALL† AND J. A. COWEN
Department of Physics, Michigan State University, East Lansing, Michigan 48823

(Received 3 August 1970)

We have made a theoretical study of the transitions induced by a magnetic field for the two-sublattice canted antiferromagnet at 0 K. The Hamiltonian for the system includes isotropic and anisotropic exchange, uniaxial single-ion anisotropy, and Dzyaloshinsky-Moriya $\mathbf{D}\cdot\mathbf{S}_1\times\mathbf{S}_2$ antisymmetric exchange. The problem is solved in the molecular-field approximation with $\mathbf{D}$ perpendicular to the antiferromagnetic easy axis. The equations of equilibrium and stability are solved numerically by computer. The antiferromagnetic to spin-flop transition occurs when the net moment reaches a critical angle $\alpha_{sh}(h_D)$. The paramagnetic transition is destroyed by the Dyzaloshinsky-Moriya (DM) interaction unless the field is applied parallel to $\mathbf{D}$. For $\mathbf{H}$ not parallel to $\mathbf{D}$, we observe a quasiparamagnetic transition which manifests itself as an inflection point in the susceptibility.

I. INTRODUCTION

Studies of the phase transitions of the uniaxial antiferromagnet have been made in the molecular-field approximation,[1,2] in the spin-wave approximation,[3] and in the Green's-function random phase approximation (RPA), and Callen decoupling approximations.[4] More recently, the canted antiferromagnet with a Dzyaloshinsky-Moriya (DM) antisymmetric exchange interaction[5] has been considered in the small-D approximation.[6–8] However, three important questions remain unresolved: (1) Does the antiferromagnetic axis undergo a true spin-flop discontinuity? (2) What are the effects of a large DM interaction? (3) What happens to the paramagnetic boundaries?

II. HAMILTONIAN

The magnetic field dependence of the phase boundaries has been studied using a Heisenberg Hamiltonian, retaining all types of second-order interaction[9]:

$$H=H_{ex}+H_{aK}+H_{aL}+H_D+H_z, \tag{1}$$

where

$$H_{ex}=\tfrac{1}{2}\sum_{ij}J_{ij}\mathbf{S}_i\cdot\mathbf{S}_j \quad \text{(isotropic exchange)}, \tag{2a}$$

$$H_{aK}=\tfrac{1}{2}\sum_{ij}K_{ij}S_i^zS_j^z \quad \text{(anisotropic exchange)}, \tag{2b}$$

$$H_{aL}=-\tfrac{1}{2}L'\sum_i[(S_i^z)^2-\tfrac{1}{3}S(S+1)] \quad \text{(uniaxial anisotropy)}, \tag{2c}$$

$$H_D=\tfrac{1}{2}\sum_{ij}D_{ij}(S_i^zS_j^x-S_i^xS_j^z) \quad \text{(DM antisymmetric exchange, } \mathbf{D}=D\hat{y}), \tag{2d}$$

$$H_z=-g\mu_B\mathbf{H}\cdot\sum_i\mathbf{S}_i \quad \text{(Zeeman interaction)}. \tag{2e}$$

The total Hamiltonian is

$$H=\tfrac{1}{2}\sum_{ij}J_{ij}\mathbf{S}_i\cdot\mathbf{S}_j+\tfrac{1}{2}\sum_{ij}K_{ij}S_i^zS_j^z-\tfrac{1}{2}L'\sum_i[(S_i^z)^2-\tfrac{1}{3}S(S+1)]+\tfrac{1}{2}\sum_{ij}D_{ij}(S_i^zS_j^x-S_i^xS_j^z)-g\mu_B\mathbf{H}\cdot\sum_i\mathbf{S}_i. \tag{3}$$

Following the formalism of Rohrer and Thomas,[2] we rewrite the Hamiltonian as a free energy in molecular fields:

$$\begin{aligned}\epsilon'=E/N=S^2[&J_1\cos(\alpha_1-\alpha_2)-\tfrac{1}{2}(L-K_2)(\cos^2\alpha_1+\cos^2\alpha_2)+K_1\cos\alpha_1\cos\alpha_2\\&+D\cos\theta\sin(\alpha_1-\alpha_2)+J_2-\tfrac{1}{3}L]\\&-g\mu_BS[H^x(\sin\alpha_1+\sin\alpha_2)\cos\theta+H^y(\sin\alpha_1+\sin\alpha_2)\sin\theta\\&+H^z(\cos\alpha_1+\cos\alpha_2)].\end{aligned} \tag{4}$$

The angles are defined according to Fig. 1. N is the number of spins per sublattice, α_1 denotes the A sublattice, $a\in A$. α_2 denotes the B sublattice, $b\in B$,

$$J_1=\sum_{a\in A}J_{ab}=\sum_{b\in B}J_{ab}, \tag{5a}$$

$$J_2=\sum_{a\in A}J_{aa'}=\sum_{b\in B}J_{bb'}, \tag{5b}$$

$$K_1=\sum_{a\in A}K_{ab}=\sum_{b\in B}K_{ab}, \tag{5c}$$

$$K_2=\sum_{a\in A}K_{aa'}=\sum_{b\in B}K_{bb'}, \tag{5d}$$

$$D=\sum_{a\in A}D_{ab}=\sum_{b\in B}D_{ab'}, \qquad D_{ab}=-D_{ba} \tag{5e}$$

$$L=L'(1-1/2S). \tag{5f}$$

We can define the molecular fields

$$H_E=J_1S/g\mu_B, \tag{6a}$$

$$H_L=(L-K_2)S/g\mu_B, \tag{6b}$$

$$H_K=K_1S/g\mu_B, \tag{6c}$$

$$H_D=DS/g\mu_B. \tag{6d}$$

We then transform the angles to a more convenient set and rewrite the energy as a dimensionless quantity.

$$\begin{aligned}\epsilon=E/NS^2J_1=&-\cos2\phi-h_L(\cos2\phi\cos^2\alpha+\sin^2\phi)\\&-h_K(\cos^2\alpha-\sin^2\phi)-h_D\cos\theta\sin2\phi\\&-2h^x\sin\phi\cos\alpha\cos\theta-2h^y\sin\phi\cos\alpha\sin\theta\\&+2h^z\sin\alpha\sin\phi,\end{aligned} \tag{7}$$

where

$$h_L=H_L/H_E, \quad \text{etc.}, \tag{8}$$

and

$$\alpha_1=\alpha+\phi, \tag{9a}$$

$$\alpha_2=\pi+\alpha-\phi. \tag{9b}$$

Our problem is now reduced to solving the equilibrium and stability equations. The equilibrium equations are

$$\partial\epsilon/\partial\eta_i=0. \tag{10}$$

The stability equations are

$$S(\eta_i, \eta_j)=(\partial^2\epsilon/\partial\eta_i^2)(\partial^2\epsilon/\partial\eta_j^2)-[\partial^2\epsilon/\partial\eta_i\partial\eta_j]^2\geq 0, \tag{11}$$

where $\boldsymbol{\eta}=(\phi, \theta, \alpha)$.

III. ZERO-TEMPERATURE PHASES

We wish to solve for the phase boundaries of a uniaxial antiferromagnet, with the z axis being the easy axis, whose xy-plane symmetry has been broken by a DM interaction with D vector in the y direction. The zero-field equilibrium configuration has both spin sublattices lying in the xz plane, "antiferromagnetically" aligned but each canted toward the x axis an angle ϕ_0, producing a net moment in the x direction.

(a) $\mathbf{h}=(0, 0, h)$ shall be referred to as the parallel or easy axis case. From symmetry we can see that $\theta=0$. The first-order transition is characterized by discontinuities in the energy or magnetization and a magnetic hysteresis. There is no unique spin-flop critical field but a region in which both the antiferromagnetic and spin-flop states are stable. The upper boundary of this region is $h_{\rm sh}$ and the lower boundary is $h_{\rm sc}$. If one increases the applied field from zero, the AF state remains stable up to $h_{\rm sh}$, analogous to the superheated liquid-gas transition. If one then reverses the process, reducing the field, the SF state remains stable down to $h_{\rm sc}$, analogous to the supercooled gas-liquid transition. The energies of the AF and SF states are equal at the thermodynamic critical field $h_{\rm th}$, implying that if $h_{\rm th}<h<h_{\rm sh}$, the AF state is metastable, and if $h_{\rm sc}<h<h_{\rm th}$, the SF state is metastable.

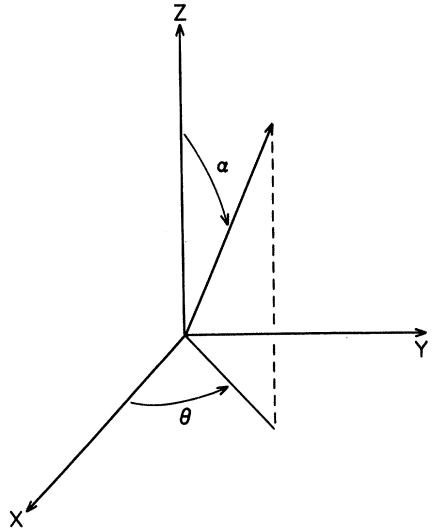

FIG. 1. Spin array with angles defined in Eq. (4).

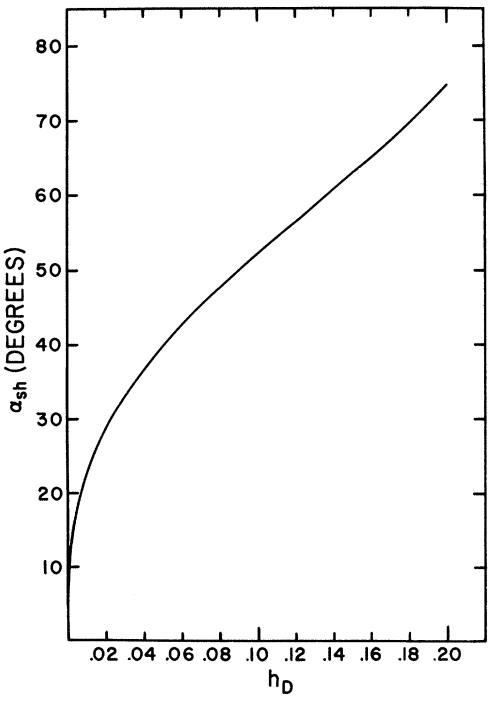

FIG. 2. Critical angle $\alpha_{\rm sh}(h_D)$ for $h_K=0$ and $h_L=0.1$ versus h_D.

The equilibrium conditions are

$$\partial\epsilon/\partial\phi=(2+h_K+h_L\cos2\alpha)\sin2\phi - 2h_D\cos2\phi+2h\sin\alpha\cos\phi=0, \tag{12}$$

$$\partial\epsilon/\partial\alpha=(h_K+h_L\cos2\phi)\sin2\alpha+2h\sin\phi\cos\alpha=0. \tag{13}$$

The stability function is

$$S(\alpha, \phi)=\{(2+h_K+h_L\cos2\alpha)\cos2\phi +2h_D\sin2\phi-h\sin\alpha\sin\phi\}\{(h_K+h_L\cos2\phi)\cos2\alpha -h\sin\alpha\sin\phi\}-\{h_L\sin2\alpha\sin2\phi-h\cos\alpha\cos\phi\}^2\geq 0. \tag{14}$$

The canting of the system in zero field is given by $h=0$, and $\alpha=0$ as

$$\tan2\phi_0=2h_D/(2+h_K+h_L). \tag{15}$$

When $\cos\alpha\neq 0$, ϕ and α are related by Eq. 13:

$$\sin\alpha=-h\sin\phi/(h_K+h_L\cos2\phi). \tag{16}$$

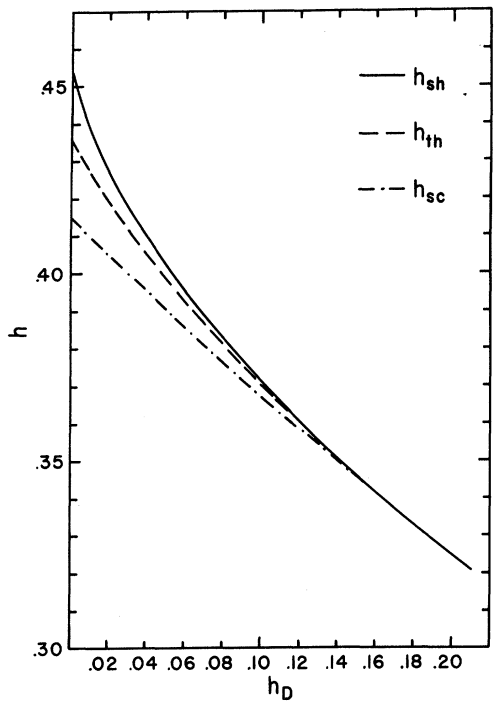

FIG. 3. Critical fields $h_{\rm th}(h_D)$, $h_{\rm sh}(h_D)$, and $h_{\rm sc}(h_D)$ versus h_D for $h_K=0$ and $h_L=0.1$.

The transition from the antiferromagnetic state to the spin-flop state, called the superheated transition, is defined by the requirement that $S(\alpha,\phi)=0$. The solution with $h_D=0$ is well known and is given by

$$h_{\rm sh}(0)=[(2+h_K+h_L)(h_K+h_L)]^{1/2}. \tag{17}$$

The $h_D=0$ case is characterized by $\alpha=0$ and $\phi=0$ for $h<h_{\rm sh}(0)$ and $\alpha=-\frac{1}{2}\pi$ for $h>h_{\rm sh}(0)$. When $h_D\neq 0$ there exists a net moment which is in the x direction in zero field but moves towards the z axis as the field is increased. Therefore, when $0<h<h_{\rm sh}(h_D)$, α and ϕ are not zero. As h approaches $h_{\rm sh}(h_D)$, $|\alpha|$ becomes larger and approaches a critical angle $\alpha_{\rm sh}(h_D)$. When h exceeds $h_{\rm sh}(h_D)$, then $\alpha=-\frac{1}{2}\pi$ and a discontinuity in magnetization has taken place. The $h_D\neq 0$ equations were solved numerically by computer using Newton's method for three unknowns (Figs. 2 and 3).

The spin-flop state is defined by letting $\alpha=-\frac{1}{2}\pi$. The boundaries for this phase occur when $S(-\frac{1}{2}\pi,\phi)=0$. When $h_D=0$, there are two phase boundaries, a spin flop to antiferromagnetic, or supercooled, boundary and a spin flop to paramagnetic boundary. The h_D solutions are

$$h_{\rm sc}(0)=(2+h_K-h_L)[(h_K+h_L)/(2+h_K+h_L)]^{1/2}, \tag{18a}$$

$$h_p^{\,||}(0)=2+h_K-h_L. \tag{18b}$$

The spin-flop state is stable, $S(-\frac{1}{2}\pi,\phi)\geq 0$, when $h_{\rm sc}(0)<h<h_p^{\,||}(0)$.

The equations with $h_D\neq 0$ were solved numerically (Fig. 3). The paramagnetic transition, which corresponds to $\phi=\frac{1}{2}\pi$ or a spin saturation, does not exist because the DM interaction will lower the energy if the spins cant slightly. To see this, examine the energy when h is large and $\phi=\frac{1}{2}\pi-\delta$, $\delta\simeq h_D/h\ll 1$:

$$\epsilon\simeq 1+h_K-h_L-2h-h_D\delta. \tag{19}$$

No matter how large h is, $\delta\neq 0$ will give a lower energy.

Experimentally, one almost always observes the thermodynamic transition defined by $\epsilon_{\rm AF}=\epsilon_{\rm SF}$. One usually argues that "nucleation centers" prevent passing of the equal energy point.[10] The procedure for finding $h_{\rm th}$ is to define

$$\Delta=\epsilon_{\rm AF}-\epsilon_{\rm SF},$$

and solve for $\Delta=0$. When $h_D=0$, the solution is

$$h_{\rm th}(0)=[(2+h_K-h_L)(h_K+h_L)]^{1/2}. \tag{20}$$

The $h_D\neq 0$ equations were solved numerically (Fig. 3). As one would expect, the critical angle $\alpha_{\rm th}$ is less than $\alpha_{\rm sh}$. The critical fields obey $h_{\rm sc}<h_{\rm th}<h_{\rm sh}$, but

$$h_{\rm th}=(h_{\rm sc}h_{\rm sh})^{1/2}$$

only when $h_D=0$.

Taking proper care to include all second-order terms, one can obtain an approximation for $h_{\rm sc}(h_D)$ where $h_D\ll 1$:

$$h_{\rm sc}(h_D)\simeq\tfrac{1}{2}\{-h_D+[h_D^2+4h_{\rm sc}^2(0)]^{1/2}\}. \tag{21}$$

Figure 4 compares Eq. (21) with the numerical results for $h_K=0$ and $h_L=0.1$.

(b) We now consider the case where $\mathbf{h}=(h,0,0)$ is perpendicular to the easy axis and the D vector. We use Eqs. (10) and (11) with $\alpha=0$ and $\theta=0$. When $h_D=0$ the paramagnetic transition occurs at

$$h_p^{\,\perp}(0)=2+h_K+h_L. \tag{22}$$

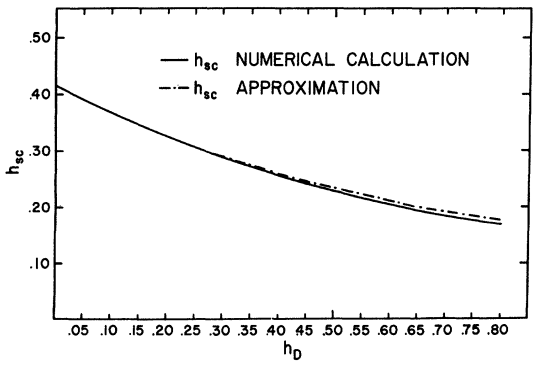

FIG. 4. Comparison of numerical value of $h_{\rm sc}(h_D)$ and Eq. (21) for $h_K=0$ and $h_L=0.1$.

As in the previous case, $h_D \neq 0$ destroys the second-order paramagnetic transition.

(c) When $\mathbf{h}=(0, h, 0)$ we are able to obtain an exact solution. For $h_D=0$ the problem is equivalent to (b). For $h_D \neq 0$,

$$\partial\epsilon/\partial\phi = (2+h_K+h_L)\sin 2\phi - 2h_D \cos 2\phi \cos\theta - 2h \cos\phi \sin\theta = 0, \quad (23)$$

$$\partial\epsilon/\partial\theta = -2h \sin\phi \cos\theta + 2h_D \sin\theta \sin\phi \cos\phi = 0, \quad (24)$$

$$S(\theta,\phi) = [(2+h_K+h_L)\cos 2\phi + 2h_D \sin 2\phi \cos\theta + h \sin\phi \sin\theta](h \sin\phi \sin\theta + h_D \cos\theta \sin\phi \cos\phi) - (h_D \sin\theta \cos 2\phi - h \cos\phi \cos\theta)^2 \geq 0. \quad (25)$$

From Eq. 24,

$$\cos\theta = (h_D/h)\cos\phi \sin\theta.$$

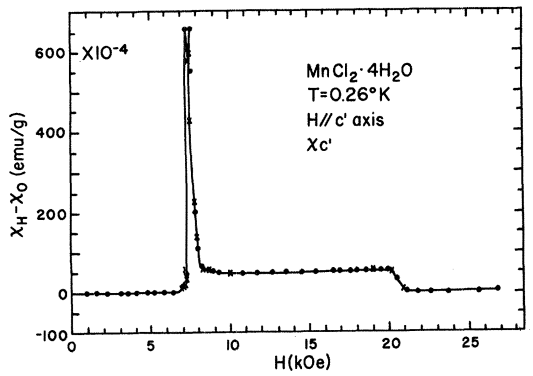

FIG. 5. $\chi^{\parallel}$ versus H for $MnCl_2 \cdot 4H_2O$. $T=0.26$ K, $H_{th}=7.5$ kG, and $H_p^{\parallel}=20.0$ kG (Ref. 11).

The solution to Eq. 23 and $S(\theta,\phi)=0$ is $\theta=\phi=\frac{1}{2}\pi$ at a critical field:

$$h_p^{\perp} = \tfrac{1}{2}\{h_p^{\perp}(0) + [(h_p^{\perp}(0))^2 + 4h_D^2]^{1/2}\}. \quad (26)$$

IV. SUSCEPTIBILITY

One method of experimentally determining the critical fields is to measure the susceptibility χ as a function of H. Rives's[11] data for χ versus H for $MnCl_2 \cdot 4H_2O$ ($h_K \simeq 0$, $h_D \simeq 0$, $h_L \simeq 0.2$) show anomalies at the spin-flop and paramagnetic boundaries (Fig. 5). For our system we can define a magnetization

$$M^x = \sin\phi \cos\alpha \cos\theta,$$
$$M^y = \sin\phi \cos\alpha \sin\theta, \quad (27)$$
$$M^z = -\sin\phi \sin\alpha.$$

The susceptibility is

$$\chi^i = dM^i/dh^i.$$

We have calculated χ^x and χ^z numerically as functions of h (Fig. 6). The zero-field susceptibility is given by

$$\chi_0^x = (\cos^2\phi_0)/(h_p^{\perp}(0)\cos 2\phi_0 + 2h_D \sin 2\phi_0), \quad (28a)$$
$$\chi_0^y = 2/(h_p^{\perp}(h_D) + h_p^{\perp}(0)), \quad (28b)$$
$$\chi_0^z = \sin^2\phi_0/(h_K + h_L \cos 2\phi_0). \quad (28c)$$

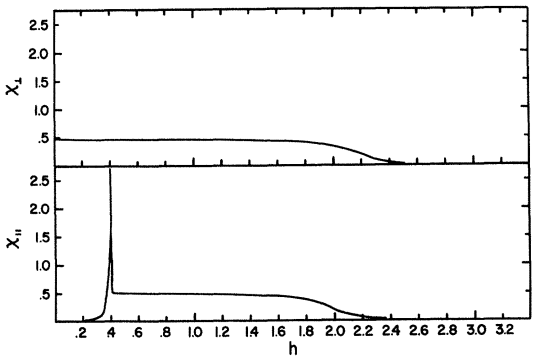

FIG. 6. Numerical calculations of χ versus h for $h_K=0$, $h_L=0.1$, and $h_D=0.05$.

The inflection point in the susceptibility corresponding to a quasiparamagnetic transition was examined by numerically calculating $d\chi/dh$ (Fig. 7) as a function of h. The x and z susceptibilities can be expressed as

$$\chi = [h_p(0) + h_D \sin\phi(4 - \cos 2\phi/\cos^3\phi)]^{-1}, \quad (29)$$

where we are assuming $h > h_{sh}(h_D)$:

$$h_p(0) = h_p^{\perp}(0) = 2 + h_K + h_L, \quad \text{for } \chi^x$$
$$= h_p^{\parallel}(0) = 2 + h_K - h_L \quad \text{for } \chi^z.$$

The quasiparamagnetic boundary is given by

$$d^2\chi^i/dh^{i2} = 0.$$

For $h_D \ll 1$ the approximate solution is

$$\cos^3\phi_{qp} \simeq (4/5)[h_D/h_p(0)], \quad (30)$$
$$h_{qp} \simeq h_p(0) + 3(h_p(0) h_D^2/100)^{1/3}. \quad (31)$$

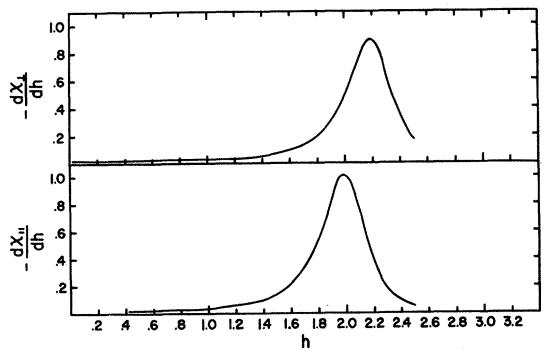

FIG. 7. Numerical calculation of $d\chi/dh$ versus h for $h_K=0$, $h_L=0.1$, and $h_D=0.05$.

For the case illustrated in Fig. 7, the numerically computed inflection points occur at

$$h_{qp}{}^{z}=1.990, \qquad \phi_{qp}{}^{z}=74.44°,$$

$$h_{qp}{}^{x}=2.195, \qquad \phi_{qp}{}^{x}=74.97°,$$

where $h_K=0$, $h_L=0.1$, $h_D=0.05$. Equations (30) and (31) give

$$h_{qp}{}^{z}=2.009, \qquad \phi_{qp}{}^{z}=74.0°,$$

$$h_{qp}{}^{x}=2.212, \qquad \phi_{qp}{}^{x}=74.5°.$$

V. CONCLUSION

The addition of a DM interaction to the uniaxial antiferromagnet with anisotropic exchange yields a Heisenberg isotropic exchange Hamiltonian with general second-order anisotropy. The hysteresis of the first-order spin-flop transition is reduced as **D** is increased and the paramagnetic transition only occurs when the field is applied parallel to **D**. Experimentally, a quasi-paramagnetic transition would be observed as an inflection point in the susceptibility for fields not parallel to **D**.

* Work supported by a National Science Foundation grant.
† NDEA Title IV Fellow.

[1] T. Nagamiya, K. Yosida, and R. Kubo, Advan. Phys. **4**, 1 (1955).
[2] H. Rohrer and H. Thomas, J. Appl. Phys. **40**, 1025 (1969).
[3] J. Feder and E. Pytte, Phys. Rev. **168**, 640 (1968).
[4] F. B. Anderson and H. B. Callen, Phys. Rev. **136**, A1068 (1964).
[5] T. Moriya, Phys. Rev. **120**, 91 (1960).
[6] G. Cinader, Phys. Rev. **155**, 453 (1966).
[7] M. S. Seehra and T. G. Castner, Phys. Rev. B **1**, 2289 (1970).
[8] K. P. Belov, A. M. Kadomtseva, and R. Z. Bevitin, Zh. Experim. i Teor. Fiz. **51**, 1306 (1966) [Soviet Phys. JETP **24**, 878 (1967)].
[9] E. F. Bertaut, in *Magnetism*, edited by G. T. Rado and H. Shul (Academic, New York, 1963) Vol. III.
[10] K. W. Blazey *et al.*, Phys. Rev. Letters **24**, 105 (1970).
[11] J. E. Rives, Phys. Rev. **162**, 491 (1967).

PHYSICAL REVIEW B VOLUME 2, NUMBER 11 1 DECEMBER 1970

Effects of Hydrostatic Pressure and of Jahn-Teller Distortions on the Magnetic Properties of $RbFeF_3$†

J. B. GOODENOUGH, N. MENYUK, K. DWIGHT, AND J. A. KAFALAS
Lincoln Laboratory, Massachusetts Institute of Technology, Lexington, Massachusetts 02173

(Received 19 June 1970)

The first-order transitions at $T_1=40°K$ and $T_2=87°K$ in $RbFeF_3$ have been measured as a function of hydrostatic pressure and applied magnetic field. It was not possible to observe the $T_N=102°K$ transition with a magnetic-susceptibility measurement. It was found that $(\Delta T_1/\Delta H_a)_p=0.35°/kOe$, $(\Delta T_2/\Delta H_a)_p=0.19°/kOe$, $(\Delta T_1/\Delta P)_H=0.18°/kbar$ and $(\Delta T_2/\Delta P)_H=-0.81°/kbar$. These results correspond to latent heats of 0.006 and 0.04 cal/g at T_1 and T_2, respectively, and relative volume changes $\Delta V_1/V_1=1.5\times10^{-6}$, $\Delta V_2/V_2=-22\times10^{-6}$. It is pointed out that a Jahn-Teller distortion to tetragonal ($c/a>1$) symmetry in the interval $T_2<T<T_N$ introduces a strong magnetoelastic coupling. This causes the heavy twinning that has been observed below T_N, and the resulting twinned structure is retained in the entire temperature interval $0<T<T_N$. In the temperature interval $T_1<T<T_2$, Rb^+-F^- interactions induce distortions to orthorhombic or tetragonal symmetries that are superimposed on the Jahn-Teller distortion. The orthorhombic distortion is cooperative across twin boundaries caused by the Jahn-Teller distortion and also permits spin canting, which introduces a ferromagnetic component below T_2. It is shown how the interplay of these distortions plus strong magnetoelastic coupling can explain the appearance of two sets of Mössbauer peaks below T_2 and results in macroscopic ferromagnetic components having cubic symmetry even though the microscopic crystallographic symmetry is "orthorhombic" ($T_1<T<T_2$). The Jahn-Teller distortion changes to rhombohedral ($\alpha<60°$) for $T<T_1$; in combination with the existing orthorhombic structure, this produces monoclinic symmetry on a microscopic scale. Nevertheless, it is shown that the macroscopic magnetization retains its cubic symmetry, that the easy magnetization direction changes from ⟨100⟩ to the ⟨110⟩, that the apparent moment increases, and that there may still be two sets of Mössbauer peaks.

I. INTRODUCTION

Above its Néel temperature $T_N=102°K$,[1] $RbFeF_3$ has the cubic perovskite structure, but it becomes tetragonal ($c/a>1$) in the interval $T_2<T<T_N$.[2] It undergoes first-order transitions at $T_1=40°K$ and $T_2=87°K$; it exhibits weak ferromagnetism at all $T<87°K$.[3] In the interval $T_1<T<T_2$, the structure appears to be orthorhombic, and below T_1 it has lower symmetry, probably monoclinic.[2] The ferromagnetic moment has a preferred direction along the pseudocubic ⟨100⟩ axes in the interval $T_1<T<T_2$, along the pseudocubic ⟨110⟩ axes below T_1.[4] It is remarkable that these noncubic crystals exhibit a cubic macroscopic anisotropy of the weak ferromagnetism. A neutron-diffraction study on a polycrystalline sample shows the dominant magnetic